Framework Expansion versus Edge Opening in a 50-e Phosphido-Bridged Triruthenium Cluster. A Case Study

Noël Lugan, Paul-Louis Fabre,[1] Dominique de Montauzon, Guy Lavigne,* and Jean-Jacques Bonnet

Laboratoire de Chimie de Coordination du CNRS, Unité associée à l'Université Paul Sabatier et à l'Institut National Polytechnique, 205, route de Narbonne, 31077 Toulouse Cedex, France

Jean-Yves Saillard and Jean-François Halet

Laboratoire de Chimie du Solide et Inorganique Moléculaire, URA CNRS 1495, Université de Rennes I, Avenue du Général Leclerc, 35042 Rennes Cedex, France

Received October 6, 1992

The electron rich cluster $Ru_3(\mu_3\text{-}\eta^2\text{-}P(C_6H_5)(C_5H_4N))(\mu\text{-}P(C_6H_5)_2)_3(CO)_6$ (**9**) is prepared by incorporation of diphenylphosphido groups into the ligand shell of triruthenium complexes that already contain a face-bridging phosphido–pyridyl ligand. The two precursors are (i) the known acyl complex $Ru_3(\mu\text{-}C(O)(C_6H_5))(\mu_3\text{-}\eta^2\text{-}P(C_6H_5)(C_5H_4N))(CO)_9$ (**1**), which reacts with 3 equiv of diphenylphosphine in refluxing methylcyclohexane to produce **9** in 75% yield, and (ii) the complex $Ru_3(\mu_3\text{-}\eta^2\text{-}P(C_6H_5)(C_5H_4N))(\mu\text{-}P(C_6H_5)_2)(CO)_6(\mu\text{-}CO)_2$ (**4**), which also leads to **9** via reaction with 2 equiv of diphenylphosphine (yield 75%). The structure of compound **9** has been determined by X-ray diffraction. Crystal data for **9**: monoclinic, C_{2h}^5, $P2_1/c$, $Z = 4$, $a = 20.246(4)$ Å, $b = 13.425(3)$ Å, $c = 20.618(4)$ Å, $\beta = 115.54(2)°$ ($T = -173$ °C), final $R = 3.7\%$ ($R_w = 4.3\%$) for 5613 unique reflections ($I \geq 3\sigma(I)$) and 310 variable parameters. The structure consists of a triangular array of ruthenium atoms capped by a phenylpyridylphosphido ligand as referred to the antecedent species. Each Ru–Ru edge is supported by a diphenylphosphido group occupying equatorial coordination sites. The environment of each Ru atom is completed by two terminal carbonyl ligands. Even though this trinuclear species contains 50 cluster valence electrons, the three Ru–Ru bond distances are roughly equivalent within experimental error: Ru(1)–Ru(2) = 3.112(1) Å, Ru(1)–Ru(3) = 3.084(1) Å, and Ru(2)–Ru(3) = 3.112(1) Å. An electrochemical study carried out in CH_2Cl_2 reveals that the compound undergoes two well-defined reversible one-electron oxidations at $E_{1/2} = 0.16$ V and $E_{1/2} = 0.53$ V, respectively (vs Ag/AgCl, KCl 0.1 M, H_2O). The unusual closed geometry of **9** is rationalized in terms of molecular orbital calculations of extended Hückel type and compared with that of the isostructural 48-e closed complex **4** and the isoelectronic 50-e open cluster $Ru_2(\mu_3\text{-}\eta^2\text{-}P(C_6H_5)(C_5H_4)(\mu\text{-}P(C_6H_5)_2)(CO)_9$ (**5**).

Introduction

Phosphido ligands have long been used as building blocks for the construction of molecular polymetallic ensembles and their stabilization.[2,3] A limitation to their use for the latter purpose has appeared through recent reports showing that opening of phosphido bridges can be induced by various chemical substrates[4,5] and is generally facile under catalytic conditions.[6,7]

In an earlier study of the complex $Ru_3(\mu_3\text{-}\eta^2\text{-}P(C_6H_5)(C_5H_4N))(\mu\text{-}P(C_6H_5)_2)(CO)_6(\mu\text{-}CO)_2$ (**4**),[8] we were led to observe for the first time a hydrogen-promoted conversion of an edge-bridging diphenylphosphido group into the terminal diphenylphosphine, leading to the complex $Ru_3(\mu\text{-}H)(\mu_3\text{-}\eta^2\text{-}P(C_6H_5)(C_5H_4N))(P(C_6H_5)_2H)(CO)_6(\mu\text{-}CO)_2$ (**8**) (eq 1).

Hydrogen activation through the above pathway was proposed as a key elementary step in the hydrogenation of cyclohexanone, catalyzed in the presence of the precursor **4**.[8] Small amounts of $Ru_3(\mu\text{-}H)(\mu_3\text{-}\eta^2\text{-}P(C_6H_5)(C_5H_4N))(CO)_9$ (**3**) and $Ru_3(\mu\text{-}H)(\mu_3\text{-}$

(1) Present address: Laboratoire de Chimie Inorganique, Université Paul Sabatier, 118 route de Narbonne, 31062 Toulouse Cedex.

(2) For leading references, see: (a) Finke, R. G.; Gaughan, G.; Pierpont, C.; Cass, M. E. *J. Am. Chem. Soc.* **1981**, *103*, 1394. (b) Carty, A. J. *Adv. Chem. Ser.* **1982**, *No. 196*, 163. (c) Carty, A. J. *Pure Appl. Chem.* **1982**, *54*, 113. (d) Rosen, R. P.; Geoffroy, G. L.; Bueno, C.; Churchill, M. R.; Ortega, R. B.; *J. Organomet. Chem.* **1983**, *254*, 89. (e) Arif, A. M.; Heaton, D. E.; Jones, R. A.; Kidd, K. B.; Wright, T. C.; Whittlesey, B. R.; Atwood, J. L.; Hunter, W. E.; Zhang, H. *Inorg. Chem.* **1987**, *26*, 4065. (f) Nucciarone, D.; MacLaughlin, S. A.; Taylor, N. J.; Carty, A. J. *Organometallics* **1988**, *7*, 106. (g) Field, J. S.; Haines, R. J.; Smit, D. N. *J. Chem. Soc., Dalton Trans.* **1988**, 1315. (h) Bullock, L. M.; Field, J. S.; Haines, R. J.; Minshall, E.; Moore, M. H.; Mulla, F.; Smit, D. N.; Steer, L. M. *J. Organomet. Chem.* **1990**, *381*, 429. (i) Braunstein, P. *New J. Chem.* **1986**, *10*, 365 and references therein. (j) Braunstein, P.; de Jesus, E.; Dedieu, A.; Lanfranchi, M.; Tiripicchio, A. *Inorg. Chem.* **1992**, *31*, 399 and references therein. (k) Braunstein, P.; de Jesus, E.; Tiripicchio, A.; Ugozzoli, F. *Inorg. Chem.* **1992**, *31*, 411 and references therein.

(3) For a recent review on bridge-assisted cluster syntheses, see: Adams, R. D. In *The Chemistry of Metal Clusters*; Shriver, D., Adams, R. D., Kaesz, H. D., Eds.; VCH: New York, 1990; Chapter 3, pp 121–170 and references therein.

(4) (a) Smith, W. F.; Taylor, N. J.; Carty, A. J. *J. Chem. Soc., Chem. Commun.* **1976**, 896. (b) Yu, Y.-F.; Gallucci, J.; Wojcicki, A. *J. Am. Chem. Soc.* **1983**, *105*, 4826. (c) Geoffroy, G. L.; Rosenberg, S.; Shulman, P. M.; Whittle, R. R. *J. Am. Chem. Soc.* **1984**, *106*, 1519. (d) Yu, Y.-F.; Chau, C.-N.; Wojcicki, A.; Calligaris, M.; Nardin, G.; Balducci, G. *J. Am. Chem. Soc.* **1984**, *106*, 3704. (e) Henrick, K.; Iggo, J. A.; Mays, M. J.; Raithby, P. R. *J. Chem. Soc., Chem. Commun.* **1984**, 209. (f) Regragui, R.; Dixneuf, P. H.; Taylor, N. J.; Carty, A. J. *Organometallics* **1984**, *3*, 814. (g) Lugan, N.; Bonnet, J.-J.; Ibers, J. A. *J. Am. Chem. Soc.* **1985**, *107*, 4484. (h) Kyba, E. P.; Davis, R. E.; Clubb, C. N.; Liu, S.-T.; Aldaz Palacios, H. O.; McKennis, J. S. *Organometallics* **1986**, *5*, 869. (i) Shyu, S.-G.; Calligaris, M.; Nardin, G.; Wojcicki, A. *J. Am. Chem. Soc.* **1987**, *109*, 3617 and references therein. (j) Shulman, P. M.; Burkhardt, E. D.; Lundquist, E. G.; Pilato, R. S.; Geoffroy, G. L. *Organometallics* **1987**, *6*, 101 and references therein.

(5) For a review, see: Lavigne, G. In *The Chemistry of Metal Clusters*; Shriver, D., Adams, R. D., Kaesz, H. D., Eds.; VCH: New York, 1990; Chapter 5, pp. 201–303 and references therein.

(6) (a) Harley, A. D.; Guskey, G. J.; Geoffroy, G. L. *Organometallics*, **1983**, *2*, 53. (b) Abatjoglou, A. G.; Billig, E.; Bryant, D. R. *Organometallics* **1984**, *3*, 923. (c) Dubois, R. A.; Garrou, P. E.; Lavin, K. D.; Allcock, H. R. *Organometallics* **1986**, *5*, 460. (d) Dubois, R. A.; Garrou, P. E. *Organometallics* **1986**, *5*, 466.

(7) For a review, see: Garrou, P. E. *Chem. Rev.* **1985**, *85*, 171 and references therein.

0020-1669/93/1332-1363$04.00/0

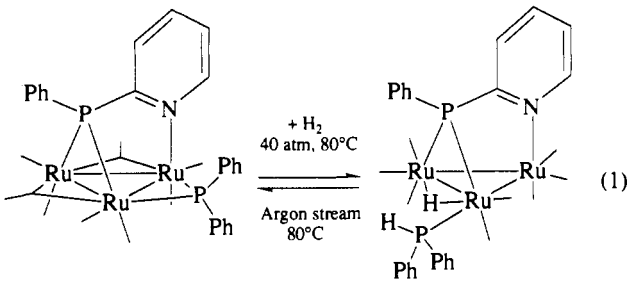

(1)

4 8

η^2-P(C_6H_5)(C_5H_4N))(μ-P(C_6H_5)$_2$)$_2$(CO)$_6$ (**7**) (existing as isomers, **7a** and **7b**) were identified in the reactor at the end of

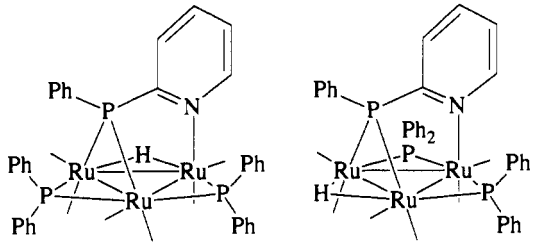

7a **7b**

catalytic runs, thereby indicating that intermolecular redistribution of PPh_2H ligands could take place as a side reaction under catalytic conditions.[8]

From the above results, there was a hint that incorporation of one more edge-bridging phosphido group into the ligand shell of the cluster might be possible. Formal replacement of a hydride ligand (one electron donor) in **7** by a phosphido group (three electron donor) might be expected to produce a 50-e species exhibiting an open structure, as found earlier for the isoelectronic complex $Ru_3(\mu_3$-η^2-P(C_6H_5)(C_5H_4N))(μ-P(C_6H_5)$_2$)(CO)$_9$ (**5**), a CO adduct of **4** (eq 2).[8]

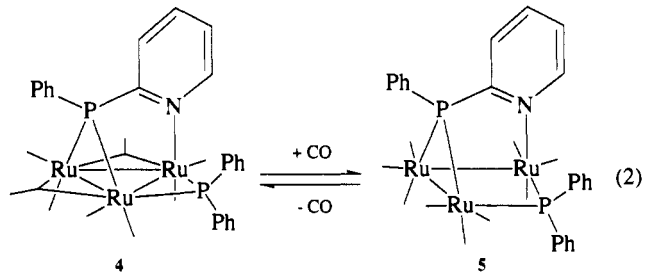

(2)

4 5

As shown in the present paper, we succeeded in the preparation of the desired species, $Ru_3(\mu_3$-η^2-P(C_6H_5)(C_5H_4N))(μ-P(C_6H_5)$_2$)$_3$(CO)$_6$ (**9**). The X ray structure analysis of this new "electron rich"[9] compound revealed that the presence of three equatorial edge-bridging phosphido ligands favors a closed vs open geometry of the metal triangle. Attempts to release electrons from the system by electrochemistry are reported. The discrepancy between the different structures shown above is rationalized in terms of molecular orbital calculations of the extended Hückel type.

Table I. Crystal and Intensity Data for $Ru_3(\mu_3$-η^2-P(C_6H_5)(C_5H_4N))(μ-P(C_6H_5)$_2$)$_3$(CO)$_6$ (**9**)

chemical formula: $C_{53}H_{39}N_1O_6P_4Ru_3$	space group; C_{2h}^5, $P2_1/c$
fw: 1213.01 amu	T = −173 °C
a = 20.246(4) Å	λ(Mo Kα_1) = 0.7093 Å
b = 13.425(3) Å	ρ_{calcd} = 1.593 g·cm^{-3}
c = 20.618(4) Å	μ = 10.406 cm^{-1}
β = 115.54(2)°	transm coeff: 0.931–0.997
V = 5056.0 Å^3	R^a = 0.037
Z = 4	$R_w{}^a$ = 0.043

^{a} $R = \sum||F_o| - |F_c||/\sum|F_o|$; $R_w = [\sum w(|F_o| - |F_c|)^2/(\sum w|F_o|^2)]^{1/2}$.

Experimental Section

General Remarks. All synthetic manipulations were performed under nitrogen or argon. Solvents were purified by standard methods. Diphenylphosphine (Aldrich) was used as received. The starting complexes $Ru_3(\mu$-C(O)(C_6H_5))(μ_3-η^2-P(C_6H_5)(C_5H_4N))(CO)$_9$ (**1**)[8b] and $Ru_3(\mu_3$-η^2-P(C_6H_5)(C_5H_4N))(μ-P(C_6H_5)$_2$)(CO)$_6$(μ-CO)$_2$ (**4**)[8a] were prepared by published procedures.

Microanalyses of C, H, N, and P elements were made by the "Service Central de Microanalyse du CNRS". Infrared spectra were recorded on a Perkin-Elmer 225 spectrophotometer using 1-mm cells equipped with CaF_2 windows. ^{31}P NMR spectra were obtained on a Bruker WH90 FT NMR spectrometer.

Preparation of $Ru_3(\mu_3$-η^2-P(C_6H_5)(C_5H_4N))(μ-P(C_6H_5)$_2$)$_3$(CO)$_6$ (9). In a typical experiment, 198 mg (1.06 mmol) of diphenylphosphine was added to a suspension of 300 mg (0.35 mmol) of $Ru_3(\mu$-C(O)(C_6H_5))(μ_3-η^2-P(C_6H_5)(C_5H_4N))(CO)$_9$ (**1**) in 30 mL of methylcyclohexane. The mixture was then heated under reflux for 3 h, during which the color of the solution turned from orange to dark red. After the mixture was cooled, the solvent was removed under vacuum. The residue was recrystallized in a mixture of dichloromethane and diethyl ether (1/2) to afford 300 mg of red crystals subsequently characterized as **9** (yield 75%).

Anal. Calcd for $C_{53}H_{39}N_1O_6P_4Ru_3$: C, 52.48; H, 3.54; N, 1.15; P, 10.21. Found C, 52.42; H, 3.54; N, 1.03; P, 10.13. IR (ν_{CO}, cm^{-1}, cyclohexane): 2030 (s), 2013 (s), 1987 (m), 1945 (m), 1940 (m), 1933 (s) cm^{-1}. IR (ν_{CO}, cm^{-1}, dichloromethane): 2028 (s), 2007 (s), 1987 (m), 1945 (sh), 1930 (s). NMR $^{31}P\{^1H\}$ ($CDCl_3$): δ 77.2 (dd, 2P, $^2J_{P1P2}$ = 15 Hz, $^2J_{P1P3}$ = 103 Hz, PPh_2), 45.0 (dt, 1P, $^2J_{P2P3}$ = 103 Hz, PPhPy), 1.4 (dt, 1P, PPh_2).

Compound **9** was also prepared from $Ru_3(\mu_3$-η^2-P(C_6H_5)(C_5H_4N))(μ-P(C_6H_5)$_2$)(μ-CO)$_2$(CO)$_6$ (**4**), in that case with 2 equiv of diphenylphosphine and under the same experimental conditions as specified above.

Crystallographic Study. Crystals of **9** suitable for X-ray diffraction were obtained by slow evaporation of a dichloromethane/diethyl ether solution at room temperature. Intensity data were recorded on an Enraf-Nonius CAD4 diffractometer at −173 °C.[10] Cell constants were obtained from a least-squares fit to the setting angles of 25 randomly selected reflections in the range 24° < 2θ(Mo Kα_1) < 28°. The space group was determined by careful examination of systematic extinctions in the listing of measured reflections. Data reductions were carried out using the SDP crystallographic computing package.[11] Table I summarizes crystal and intensity data.

The structure was solved by using the SDP crystallographic computing package and refined by using the SHELX-76 package.[12] The position of Ru and P atoms was determined by direct methods. All remaining non-hydrogen atoms were located by the usual combination of full matrix least-squares refinement and difference electron density syntheses.

Atomic scattering factors were taken from the usual tabulations.[13] Anomalous dispersion terms for Ru and P atoms were included in F_c.[14] An empirical absorption correction was applied.[15] All non-hydrogen atoms

(8) (a) Lugan, N.; Lavigne, G.; Bonnet, J.-J.; Réau, R.; Neibecker, D.; Tkatchenko, I. *J. Am. Chem. Soc.* **1988**, *110*, 5369, and references therein. (b) Lugan, N.; Lavigne, G.; Bonnet, J.-J. *Inorg. Chem.* **1987**, *26*, 585. (c) For comparative purposes, the label numbers used for the known compounds in the present paper are the same as in the previous one, ref 8a.

(9) (a) The term was coined by Adams[9b] and also applies to early examples[9c-e] in which simultaneous expansion of all metal–metal bonds was found to reflect a tendency to reduce the antibonding character. Other relevant examples are also provided later in this article. (b) Adams, R. D.; Yang, L.-W. *J. Am. Chem. Soc.* **1983**, *105*, 235. (c) Frisch, P. D.; Dahl, L. F. *J. Am. Chem. Soc.* **1972**, *94*, 5082. (d) Kamijo, N.; Watanabe, T. *Acta Crystallogr.* **1979**, *B35*, 2537. (e) Wei, C.-H.; Dahl, L. F. *Inorg. Chem.*, **1965**, *4*, 493.

(10) Low-temperature device designed by J.-J. Bonnet and S. Askenazy. Commercially available from Soterem Z. I. de Vic, 31320 Castanet-Tolosan, France.

(11) *Enraf-Nonius Structure Determination Package*; 4th ed.; B. A. Frenz & Associates, Inc.: College Station, TX, and Enraf-Nonius: Delft, The Netherlands, 1981.

(12) Sheldrick, G. M. *SHELX-76, Program for Crystal Structure Determination*; University of Cambridge: Cambridge, England, 1976.

were allowed to vibrate anisotropically, except carbon atoms of the phenyl rings which were refined as isotropic rigid groups (idealized D_{6h} symmetry; C–C = 1.395 Å) in order to reduce the number of variable parameters. Hydrogen atoms were entered in idealized positions (C–H = 0.97 Å) riding the carbon atoms. Scattering factors for the hydrogen atoms were taken from Stewart et al.[16]

Final atomic coordinates and $U_{eq} \times 100$ (or $U_{iso} \times 100$) for non-hydrogen atoms are given in Table II. A table of anisotropic thermal parameters and a listing of observed and calculated structure factor amplitudes ($10|F_o|$ vs $10|F_c|$) are provided as supplementary material.

Electrochemical Study. Electrochemical measurements were carried out using a laboratory made potentiostat controlled by an Apple II microcomputer. This apparatus allows automatic *iR* drop correction, which is necessary in CH_2Cl_2.[17] The electrochemical cell was a conventional one with three electrodes: reference, Ag/AgCl, KCl 10^{-1}M, H_2O; working, Pt disk (3.14 mm^2); auxiliary, Pt wire. The supporting electrolyte NBu_4PF_6 0.1 M (Fluka, purum) was used without further purification. CH_2Cl_2 (Merck, analytical grade) was passed over alumina before use. All experiments were carried out under argon. ESR spectra were recorded in frozen solution (110 K), after exhaustive potential controlled oxidation, on a Bruker ER 200-D spectrometer using a conventional X-band (9.63 GHz) accessory. Electronic absorption spectra were recorded on a Cary 2300 spectrophotometer.

EHMO Calculations. Calculations were carried out within the extended Hückel formalism,[18] using the weighted H_{ij} formula.[19] Standard atomic parameters were taken for H, C, N, O,[18] and P.[20] The exponent (ζ) and the valence shell ionization potential (H_{ii} in eV) for Ru were as follows, respectively: 2.078, –8.60 for 5s; 2.043, –5.10 for 5p. The H_{ii} value for 4d was set equal to –12.20. A linear combination of two Slater-type orbitals (ζ_1 = 5.378, c_1 = 0.5540; ζ_2 = 2.303, c_2 = 0.6365) was used to represent the atomic d orbitals. Calculations were based on idealized structures of compounds **4**, **5**, and **9**. In models **A**, **B**, and **C**, the following atomic distances (Å) were used: Ru–Ru = 3.10, Ru–C = 1.88, and C–O = 1.14. The C–Ru–C angles were set at 90°. In **C**, the nonbonding Ru–Ru contact was 3.80 Å.

Results and Discussion

Preparation of the Complex. The complex $Ru_3(\mu_3\text{-}\eta^2\text{-}P(C_6H_5)(C_5H_4N))(\mu\text{-}P(C_6H_5)_2)_3(CO)_6$ (**9**) is formally the result of a replacement of two equatorial bridging carbonyl ligands of the antecedent species $Ru_3(\mu_3\text{-}\eta^2\text{-}P(C_6H_5)(C_5H_4N))(\mu\text{-}P(C_6H_5)_2)(CO)_6(\mu\text{-}CO)_2$ (**4**) by two diphenylphosphido groups. Such a substitution was found to take place straightforwardly in the presence of diphenylphosphine in refluxing cyclohexane, with concomittant elimination of CO and H_2 (eq 3). Given that the

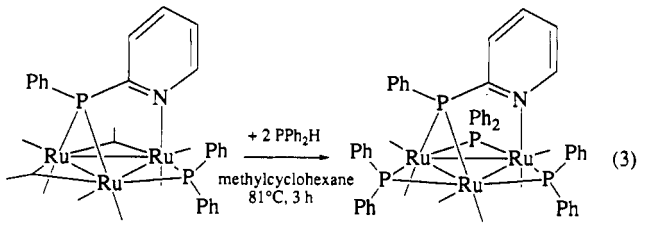

4 9 (3)

starting complex of the above reaction is derived from the antecedent acyl complex $Ru_3(\mu\text{-}C(O)(C_6H_5))(\mu_3\text{-}\eta^2\text{-}P(C_6H_5)(C_5H_4N))(CO)_9$ (**1**) by addition of 1 equiv of diphenylphosphine,

Table II. Fractional Atomic Coordinates and Isotropic or Equivalent Temperature Factors ($Å^2 \times 100$) with esd's in Parentheses (U_{eq} = $^1/_3$ Trace **U**)

atom	x/a	y/b	z/c	U_{eq}/U_{iso}
Ru(1)	0.16569(3)	0.01357(4)	0.78540(2)	1.07(3)
Ru(2)	0.22747(3)	0.17868(4)	0.72085(3)	1.13(3)
Ru(3)	0.32440(3)	–0.00146(4)	0.80246(3)	1.13(3)
P(1)	0.30716(8)	0.1567(1)	0.84453(8)	1.23(8)
P(2)	0.11685(8)	0.1670(1)	0.73092(8)	1.32(8)
P(3)	0.33637(9)	0.1147(1)	0.72119(9)	1.37(8)
P(4)	0.26135(9)	–0.0957(1)	0.85403(9)	1.33(8)
C(1)	0.1455(3)	–0.0583(5)	0.7018(4)	1.7(4)
O(1)	0.1341(3)	–0.1048(4)	0.6509(3)	2.8(3)
C(2)	0.0813(4)	–0.0318(5)	0.7914(3)	1.7(4)
O(2)	0.0275(3)	–0.0569(4)	0.7912(3)	3.0(3)
C(3)	0.1716(4)	0.1545(5)	0.6202(4)	2.1(4)
O(3)	0.1390(3)	0.1436(4)	0.5597(2)	2.7(3)
C(4)	0.2335(3)	0.3136(5)	0.7058(3)	1.8(4)
O(4)	0.2357(3)	0.3970(4)	0.6943(3)	3.6(3)
C(5)	0.3128(3)	–0.1114(5)	0.7391(3)	1.7(4)
O(5)	0.3071(3)	–0.1767(4)	0.7017(3)	2.7(3)
C(6)	0.4199(4)	–0.0325(5)	0.8645(4)	1.9(4)
O(6)	0.4790(3)	–0.0537(4)	0.9036(3)	2.7(3)
N(1)	0.2033(3)	0.0978(4)	0.8845(3)	1.3(3)
C(21)	0.2630(3)	0.1571(5)	0.9051(3)	1.2(3)
C(22)	0.2864(4)	0.2149(5)	0.9673(3)	1.8(4)
C(23)	0.2497(4)	0.2110(5)	1.0099(4)	2.1(4)
C(24)	0.1897(4)	0.1487(5)	0.9893(3)	2.4(4)
C(25)	0.1684(3)	0.0935(5)	0.9274(3)	1.9(4)
C(11)	0.3870(2)	0.2356(2)	0.8942(2)	1.5(1)
C(12)	0.4470(2)	0.1935(2)	0.9512(2)	2.0(2)
C(13)	0.5092(2)	0.2509(2)	0.9897(2)	2.5(2)
C(14)	0.5114(2)	0.3504(2)	0.9711(2)	2.2(2)
C(15)	0.4513(2)	0.3925(2)	0.9141(2)	2.1(2)
C(16)	0.3891(2)	0.3351(2)	0.8757(2)	1.8(1)
C(31)	0.0335(2)	0.1733(3)	0.6463(2)	1.6(1)
C(32)	0.0040(2)	0.2667(3)	0.6196(2)	3.0(2)
C(33)	–0.0564(2)	0.2744(3)	0.5530(2)	3.7(2)
C(34)	–0.0874(2)	0.1887(3)	0.5131(2)	2.8(2)
C(35)	–0.0579(2)	0.0954(3)	0.5398(2)	4.0(2)
C(36)	0.0025(2)	0.0877(3)	0.6065(2)	3.5(2)
C(41)	0.0893(2)	0.2445(3)	0.7881(2)	1.6(1)
C(42)	0.0258(2)	0.2168(3)	0.7941(2)	2.1(2)
C(43)	0.0064(2)	0.2653(3)	0.8433(2)	2.4(2)
C(44)	0.0505(2)	0.3414(3)	0.8863(2)	2.7(2)
C(45)	0.1140(2)	0.3690(3)	0.8803(2)	2.9(2)
C(46)	0.1334(2)	0.3206(3)	0.8311(2)	2.0(2)
C(51)	0.4135(2)	0.2028(3)	0.7491(2)	1.8(1)
C(52)	0.4017(2)	0.2967(3)	0.7171(2)	2.1(2)
C(53)	0.4585(2)	0.3661(3)	0.7394(2)	2.4(2)
C(54)	0.5270(2)	0.3416(3)	0.7937(2)	2.6(2)
C(55)	0.5388(2)	0.2477(3)	0.8257(2)	2.8(2)
C(56)	0.4820(2)	0.1783(3)	0.8034(2)	2.2(2)
C(61)	0.3324(2)	0.0666(3)	0.6359(2)	1.8(1)
C(62)	0.2753(2)	0.0031(5)	0.5944(2)	2.2(2)
C(63)	0.2707(2)	–0.0334(3)	0.5292(2)	2.9(2)
C(64)	0.3232(2)	–0.0063(3)	0.5056(2)	3.1(2)
C(65)	0.3803(2)	0.0573(3)	0.5472(2)	2.9(2)
C(66)	0.3849(2)	0.0938(3)	0.6123(2)	2.1(2)
C(71)	0.2485(2)	–0.2294(3)	0.8338(3)	1.7(1)
C(72)	0.1808(2)	–0.2737(3)	0.8173(3)	2.8(2)
C(73)	0.1718(2)	–0.3760(3)	0.8045(3)	3.4(2)
C(74)	0.2305(2)	–0.4339(3)	0.8082(3)	3.3(2)
C(75)	0.2982(2)	–0.3896(3)	0.8246(3)	2.8(2)
C(76)	0.3072(2)	–0.2873(3)	0.8375(3)	2.1(2)
C(81)	0.2863(2)	–0.0958(3)	0.9513(2)	1.5(1)
C(82)	0.2442(2)	–0.1492(3)	0.9780(2)	2.6(2)
C(83)	0.2576(2)	–0.1396(3)	1.0499(2)	3.3(2)
C(84)	0.3130(2)	–0.0765(3)	1.0953(2)	2.9(2)
C(85)	0.3551(2)	–0.0231(3)	1.0687(2)	2.3(2)
C(86)	0.3418(2)	–0.0327(3)	0.9967(2)	1.9(1)

the simplest synthetic procedure, a one-pot synthesis, involves addition of 3 equiv of diphenylphosphine to a cyclohexane solution of **1**, heated under reflux. Evidence for the formation of benzaldehyde during the latter reaction was obtained by GC analysis of the crude solution. Complex **9** was isolated in 75% yield after recrystallization. ^{31}P NMR data are consistent with

(13) Cromer, D. T.; Waber, J. T. *International Tables for X-ray Crystallography*; Kynoch Press: Birmingham, England, 1974, Vol 4, Table 2.2B.
(14) Cromer, D. T.; Waber, J. T. *International Tables for X-ray Crystallography*; Kynoch Press: Birmingham, England, 1974, Vol 4, Table 2.3.1.
(15) North, A. C. T.; Phillips, D. C.; Mathews, F. S. *Acta Crystallogr.* **1968**, *A24*, 351.
(16) Stewart, R. F.; Davidson, E. R.; Simpson, W. T. *J. Chem. Phys.* **1965**, *42*, 3175.
(17) Cassoux, P.; Dartiguepeyron, R.; Fabre, P.-L.; de Montauzon, D. *Electrochim. Acta* **1985**, *30*, 1485.
(18) Hoffmann, R. *J. Chem. Phys.* **1963**, *39*, 1397.
(19) Ammeter, J. H.; Bürgi, H.-B.; Thibeault, J.; Hoffmann, R. *J. Am. Chem. Soc.* **1978**, *100*, 3686.
(20) Summerville, R. H.; Hoffmann, R. *J. Am. Chem. Soc.* **1976**, *98*, 7240.

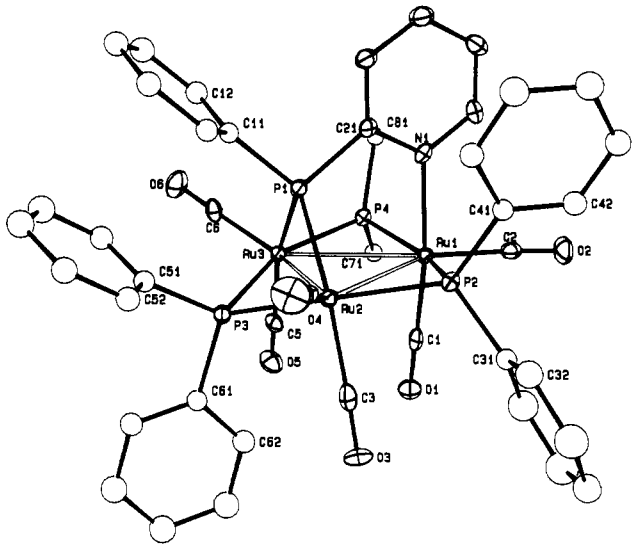

Figure 1. Perspective view of the complex $Ru_3(\mu_3\text{-}\eta^2\text{-}PPhpy)(\mu\text{-}PPh_2)_3(CO)_6$ (**9**). The thermal ellipsoids are shown at the 50% probability level. The two phenyl substituents attached to P(4) have been omitted for clarity.

Table III. Interatomic Distances (Å) for $Ru_3(\mu_3\text{-}\eta^2\text{-}P(C_6H_5)(C_5H_4N))(\mu\text{-}P(C_6H_5)_2)_3(CO)_6$ (**9**), with Esd's in Parentheses

Ru(1)–Ru(2)	3.112(1)	Ru(3)–C(6)	1.848(7)
Ru(1)–Ru(3)	3.084(1)	P(1)–C(11)	1.832(4)
Ru(1)–P(2)	2.351(2)	P(1)–C(21)	1.822(9)
Ru(1)–P(4)	2.354(2)	P(2)–C(31)	1.832(4)
Ru(1)–N(1)	2.166(6)	P(2)–C(41)	1.830(6)
Ru(1)–C(1)	1.861(8)	P(3)–C(51)	1.842(4)
Ru(1)–C(2)	1.868(9)	P(3)–C(61)	1.841(6)
Ru(2)–Ru(3)	3.112(1)	P(4)–C(71)	1.836(5)
Ru(2)–P(1)	2.376(2)	P(4)–C(81)	1.846(5)
Ru(2)–P(2)	2.342(2)	N(1)–C(21)	1.35(1)
Ru(2)–P(3)	2.363(2)	N(1)–C(25)	1.35(1)
Ru(2)–C(3)	1.915(7)	C(21)–C(22)	1.40(1)
Ru(2)–C(4)	1.850(7)	C(22)–C(23)	1.37(2)
Ru(3)–P(1)	2.376(2)	C(23)–C(24)	1.38(1)
Ru(3)–P(3)	2.376(2)	C(24)–C(25)	1.38(1)
Ru(3)–P(4)	2.351(3)	⟨C–O⟩[a]	1.14[2]
Ru(3)–C(5)	1.917(8)		

[a] Within carbonyl groups.

the approximate C_s symmetry of the complex found in the solid-state structure (vide infra). The doublet of doublets appearing at 77.2 ppm can be unambigously attributed to two diphenylphosphido groups spanning the two equivalent edges of the metal triangle. Taking into account the J_{PP} values and by analogy with the ^{31}P NMR spectra of the compound $Ru_3(\mu\text{-}H)(\mu_3\text{-}\eta^2\text{-}P(C_6H_5)(C_5H_4N))(\mu\text{-}P(C_6H_5)_2)_2(CO)_6$ (**7**),[8a] the doublets of triplets located at 45.0 ppm and 1.4 ppm are respectively attributed to the phenylpyridylphosphido group and to the unique diphenylphosphido ligand.

Description of the Structure. A perspective view of complex **9** is shown in Figure 1. Selected interatomic distances and bond angles are given in Tables III and IV, respectively.

The structure consists of a triangular array of ruthenium atoms, capped by a phenylpyridylphosphido ligand via (i) the nitrogen atom N(1) of the pyridyl ring, bound to Ru(1) (Ru(1)–N(1) = 2.166(6) Å), and (ii) the phosphorus atom P(1), symmetrically bridging the Ru(2)–Ru(3) edge (Ru(2)–P(1) = 2.376(2) Å; Ru(3)–P(1) = 2.376(2) Å). Each of the three edges of the metal triangle is supported by a diphenylphosphido group. The corresponding phosphorus atoms P(2), P(3), and P(4) are close to the plane of the metal triangle (P(2)–{Ru(1)–Ru(2)–Ru(3)} = –0.210(2) Å; P(3)–{Ru(1)–Ru(2)–Ru(3)} = +0.555(2) Å; P(4)–{Ru(1)–Ru(2)–Ru(3)} = –0.274(2) Å). The smallest nonbonding P···P distance is found between P(1) and P(3) (P(1)···P(3) = 2.904(3) Å). The environment of each Ru atom

Table IV. Selected Bond Angles (deg) for $Ru_3(\mu_3\text{-}\eta^2\text{-}P(C_6H_5)(C_5H_4N))(\mu\text{-}P(C_6H_5)_2)_3(CO)_6$ (**9**) with Esd's in Parentheses

Ru(2)–Ru(1)–Ru(3)	60.27(2)	P(1)–Ru(2)–C(4)	103.8(2)
Ru(2)–Ru(1)–P(2)	48.31(6)	P(2)–Ru(2)–P(3)	154.42(7)
Ru(2)–Ru(1)–P(4)	108.84(6)	P(2)–Ru(2)–C(3)	86.8(3)
Ru(2)–Ru(1)–N(1)	89.4(2)	P(2)–Ru(2)–C(4)	102.4(3)
Ru(2)–Ru(1)–C(1)	86.6(3)	P(3)–Ru(2)–C(3)	93.2(3)
Ru(2)–Ru(1)–C(2)	143.9(2)	P(3)–Ru(2)–C(4)	103.2(3)
Ru(3)–Ru(1)–P(2)	108.31(6)	C(3)–Ru(2)–C(4)	92.0(3)
Ru(3)–Ru(1)–P(4)	49.03(6)	Ru(1)–Ru(3)–Ru(2)	60.29(2)
Ru(3)–Ru(1)–N(1)	90.1(2)	Ru(1)–Ru(3)–P(1)	70.94(5)
Ru(3)–Ru(1)–C(1)	82.6(3)	Ru(1)–Ru(3)–P(3)	107.13(5)
Ru(3)–Ru(1)–C(2)	155.3(5)	Ru(1)–Ru(3)–P(4)	49.12(5)
P(2)–Ru(1)–P(4)	154.26(7)	Ru(1)–Ru(3)–C(5)	99.0(3)
P(2)–Ru(1)–N(1)	84.1(2)	Ru(1)–Ru(3)–C(6)	145.2(3)
P(2)–Ru(1)–C(1)	97.6(3)	Ru(2)–Ru(3)–P(1)	49.06(4)
P(2)–Ru(1)–C(2)	96.2(3)	Ru(2)–Ru(3)–P(3)	48.77(5)
P(4)–Ru(1)–N(1)	83.9(2)	Ru(2)–Ru(3)–P(4)	108.94(5)
P(4)–Ru(1)–C(1)	91.7(2)	Ru(2)–Ru(3)–C(5)	111.5(2)
P(4)–Ru(1)–C(2)	107.2(3)	Ru(2)–Ru(3)–C(6)	141.0(3)
N(1)–Ru(1)–C(1)	172.8(3)	P(1)–Ru(3)–P(3)	75.26(7)
N(1)–Ru(1)–C(2)	93.8(3)	P(1)–Ru(3)–P(4)	97.06(7)
C(1)–Ru(1)–C(2)	93.0(4)	P(1)–Ru(3)–C(5)	160.5(2)
Ru(1)–Ru(2)–Ru(3)	59.44(2)	P(1)–Ru(3)–C(6)	102.9(3)
Ru(1)–Ru(2)–P(1)	70.44(8)	P(3)–Ru(3)–P(4)	155.82(6)
Ru(1)–Ru(2)–P(2)	49.11(5)	P(3)–Ru(3)–C(5)	92.6(3)
Ru(1)–Ru(2)–P(3)	106.61(5)	P(3)–Ru(3)–C(6)	104.0(3)
Ru(1)–Ru(2)–C(3)	100.6(3)	P(4)–Ru(3)–C(5)	87.9(3)
Ru(1)–Ru(2)–C(4)	146.7(3)	P(4)–Ru(3)–C(6)	100.1(3)
Ru(3)–Ru(2)–P(1)	49.12(5)	C(5)–Ru(3)–C(6)	94.7(3)
Ru(3)–Ru(2)–P(2)	107.71(5)	Ru(2)–P(1)–Ru(3)	81.75(6)
Ru(3)–Ru(2)–P(3)	49.10(5)	Ru(1)–P(2)–Ru(2)	83.14(6)
Ru(3)–Ru(2)–C(3)	113.2(3)	Ru(2)–P(3)–Ru(3)	82.03(8)
Ru(3)–Ru(2)–C(4)	141.2(2)	Ru(1)–P(4)–Ru(3)	81.85(6)
P(1)–Ru(2)–P(2)	97.40(7)	P(1)–C(21)–N(1)	114.8(5)
P(1)–Ru(2)–P(3)	75.63(7)	⟨Ru–C–O⟩[a]	177.7[9]
P(1)–Ru(2)–C(3)	162.32(7)		

[a] Within carbonyl groups.

is completed by two terminal carbonyl ligands. Among axial carbonyl ligands, those being trans to P(1) display the longest Ru–C bond length, in agreement with the expected trans influence ascribed to phosphorus. The orientation of all three equatorial carbonyl ligands C(2)O(2), C(4)O(4), and C(6)O(6), is such that the C–Ru vectors point toward the center of the metal triangle (in planar projection). Thus, the overall ligand distribution is closely related to that found in the antecedent species $Ru_3(\mu_3\text{-}\eta^2\text{-}P(C_6H_5)(C_5H_4N))(\mu\text{-}P(C_6H_5)_2)(CO)_6(\mu\text{-}CO)_2$[8a] or in the tris-edge-bridged complex $Ru_3(\mu\text{-}H)(\mu\text{-}P(C_6H_5)_2)_3(CO)_7$ originally reported by Geoffroy, Churchill, and co-workers[2d] and also crystallized later in a different crystal system by Haines et al.[2h]

On the basis of the 18-e rule, the metal triangle of the 50-e cluster **9** would be expected to exhibit an "open" geometry, with only *two* direct Ru–Ru bonds. In fact, the three metal–metal distances are roughly equivalent, and a global expansion is observed: Ru(1)–Ru(2) = 3.112(1) Å; Ru(1)–Ru(3) = 3.084(1) Å; Ru(2)–Ru(3) = 3.112(1) Å. These values are 0.12 Å longer than those found for $Ru_3(\mu\text{-}H)(\mu\text{-}P(C_6H_5)_2)_3(CO)_7$,[2d,2h,21] the closest 48-e species also bearing three edge-bridging phosphido groups.

Only a few 50-e cluster compounds exhibiting an expanded framework of a closed type are known. The first ones, $Os_3(\mu\text{-}\eta^2\text{-}C{\equiv}CR)_2(\mu\text{-}PPh_2)_2(CO)_7$, and $Os_3(\mu\text{-}\eta^2\text{-}C{\equiv}CPh)_2(\eta^1\text{-}C{\equiv}CPh)(\mu\text{-}PPh_2)_2(EtNH_2)(CO)_6$, were reported by Carty et al.,[22] who noted a striking resemblance between the frontier orbitals of such compounds and those of $[Pt_3(CO)_3(\mu_2\text{-}PH_2)_3]^+$.[23] While

(21) The average value obtained by Churchill[2d] for the phosphido-bridged metal–metal edges in the 48-e compound $Ru_3(\mu\text{-}H)(\mu\text{-}P(C_6H_5)_2)_3(CO)_7$ was found to be 2.985 Å (data taken from two crystallographically independent cluster units A and B in the lattice: Ru(1)–Ru(2) = 2.964(1) Å and Ru(1)–Ru(3) = 2.965(1) Å for molecule A, and Ru(1)–Ru(2) = 2.977(1) Å and Ru(1)–Ru(3) = 3.033(1) Å for molecule B. The above average value does not take into account the doubly bridged edge (μ-hydrido, μ-phosphido): ⟨Ru(2)–Ru(3)⟩ = 2.807 Å.

(22) Cherkas, A. A.; Taylor, N. J.; Carty, A. J. *J. Chem. Soc., Chem. Commun.* **1990**, 385.

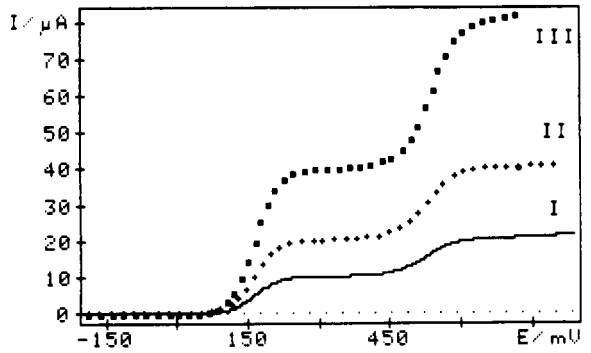

Figure 2. Rotating disk electrode voltammetry of complex **9**. Concentration varies from 0.5×10^{-4} to 2×10^{-3} M in CH_2Cl_2 containing 0.1 M NBu_4PF_6; Pt electrode; rotating speed ω = 2000 rpm; scan rate v = 4 mV·s^{-1}; V vs Ag/AgCl, 0.1 M KCl.

Table V. Voltamperometry Characteristics of Complex 9 under Diffusion Control in CH_2Cl_2, Containing 0.1 M NBu_4PF_6, at a Platinum Electrode[a]

	first step			second step		
cluster concn (M)	$E_{1/2}$ (mV)	I_d (μA)	p (mV)[b]	$E_{1/2}$ (mV)	I_d (μA)	p (mV)
0.5×10^{-3}	164	10.0	57	525	9.9	67
1.0×10^{-3}	163	20.0	57	529	19.5	61
2.0×10^{-3}	165	39.3	56	535	38.4	59

[a] Rotation speed = 2000 rpm. [b] p = regression slope of $\log |(I_d - I)/I|$.

we were in the process of submitting our work, an even more relevant compound, $Ru_3(\mu\text{-}Cl)(\mu\text{-}P(C_6H_5)_2)_3(CO)_7$, was reported by Cabeza et al. in a preliminary communication.[24] In the latter complex, a bridging halide and a carbonyl group are seen to occupy respectively the same coordination sites as the phosphorus and nitrogen atoms of the phosphidopyridyl ligand in **9**.

Since the expanded metal framework of **9** was indicative of an excess of electrons, we became interested in the synthesis of the corresponding oxidized species by electrochemistry.

Electrochemistry. In dichloromethane solution, complex **9** is electroactive at a platinum electrode. The cluster undergoes two well-defined reversible monoelectronic oxidations at $E_{1/2}$ = 0.16 V and $E_{1/2}$ = 0.53 V, respectively (Figure 2, Table V).

Potential controlled coulometry and comparisons between the RDE limiting currents corresponding to the oxidation steps of the cluster and to the oxidation of ferrocene both indicate that the complex undergoes two one-electron oxidation, with the following characteristics for each reduction step:

(i) Under stationary conditions, the limiting current $I_d = f(c)$ is a straight line crossing the origin of the axes. The plot $1/I_d = f(1/\omega^{1/2})$ has similar characteristics (ω = angular rotation frequency). Thus, the limiting current is diffusion controlled.

(ii) Under nonstationary conditions, the current peak ratio $I_{pc}/I_{pa} \approx 1$ for potential sweep rate $0.1 \leq v \leq 9$ V·s^{-1} (Figure 3, Table VI), $I_{pa} = f(v^{1/2})$, is a straight line crossing the origin of the axes. Thus, the two oxidation steps are electrochemically reversible.

Under diffusion control, the limiting current, linearly related to concentration and $\omega^{1/2}$, allows us to calculate the diffusion coefficient of the complex from Levich's equation: $D^0 = 4.6 \times 10^{-6}$ cm^2·s^{-1}.

Cyclic voltammetry results lead to the determination of the standard heterogenous rate constant k_0 calculated for the two oxidation steps. This constant is 9×10^{-3} cm·s^{-1} for the first step and 7×10^{-3} cm·s^{-1} for the second one.[25] The values of $\Delta G^{\ddagger}$ = 8.26 K·cal·mol^{-1} and 8.41 K·cal·mol^{-1} calculated as described by

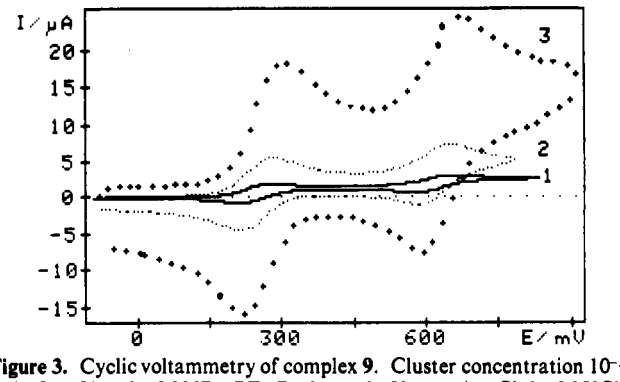

Figure 3. Cyclic voltammetry of complex **9**. Cluster concentration 10^{-3} M in CH_2Cl_2 + 0.1 M NBu_4PF_6; Pt electrode; V vs Ag/AgCl, 0.1 M KCl; scan rate v = 0.01 (+), 0.1(●), 1(—) V·s^{-1}.

Table VI. Voltamperometry Characteristics of Complex 9 by Cyclic Voltammetry in CH_2Cl_2 Containing 0.1 M NBu_4PF_6, at a Platinum Electrode[a]

	first step				second step			
scan rate (V·s^{-1})	E_{pa} (mV)	I_{pa} (μA)	RI_p	ΔE_p (mV)	E_{pa} (mV)	I_{pa} (μA)	RI_p	ΔE_p (mV)
0.1	202	5.7	1	68	575	6.0	0.97	66
1	210	16.8	0.98	81	587	17.2	0.99	82
9	225	44.0	0.93	127	620	46.5	0.99	125

[a] ΔE_p = peak separation (E_p(forward) − E_p(backward)) = $E_{p(ox)} - E_{p(red)}$. RI_p = $|I_p$ backward/I_p forward$|$.

Marcus[26] from the k_0 obtained in oxidation ($k_0 = KZ \exp(-\Delta G^{\ddagger}/RT)$ is reasonably close to that of $\Delta G^{\ddagger}$ previously determined (8 K·cal·mol^{-1}) for the electron transfer to the tetranuclear clusters $Co_4(CO)_{12-n}(Ph_2PCH_2PPh_2)_n$ (n = 0, 1, 2).[27]

After controlled potential electrolysis at +0.6 V of the solution of **9**, a paramagnetic species was obtained, as indicated by an ESR signal (g = 2.116) with no hyperfine structure at 100 K. The IR spectrum of the resultant pink solution ν_{CO} = 2052 (s), 2031 (s), 2020 (m), 1990 (m br), 1975 (sh) cm^{-1} indicates that electrochemical oxidation takes place with the formation of the monocationic species. The following scheme is proposed for this first oxidation reaction:

$$Ru_3P_4 \rightleftharpoons [Ru_3P_4]^+ + e^-$$

Electrolysis carried out at +1.0 V on the second plateau on a solution of **9** generated an ESR-inactive species. This yellow-brown species is also characterized by IR absorption bands ν_{CO} = 2051, 2019 cm^{-1}, suggesting that this complex has been decomposed into nonidentified products. Nevertheless, after exhaustive electrolysis either at 0.6 or 1.0 V, it was impossible to regenerate the starting material by inverse coulometry, although both oxidations were electrochemically and chemically reversible on the time scale of the cyclic voltammetry experiment.

The coulometric oxidation was also monitored by UV spectroscopy. During the first step of the electrolysis, the initial absorption band in the electronic spectrum at 387 nm was found to disappear progressively, with concomitant formation of a new peak at 447 nm. This provided evidence for the formation of the monocationic species with retention of the initial skeleton. The fate of this peak during the second step, not followed by the appearance of a new one, confirmed decomposition of the monocationic species.

Theoretical Analysis. As previously mentioned, the complex $Ru_3(\mu_3\text{-}\eta^2\text{-}P(C_6H_5)(C_5H_4N))(\mu\text{-}CO)_2(\mu\text{-}P(C_6H_5)_2)(CO)_6$ (**4**), possesses 48 CVE's and obeys the 18-electron rule. This cluster

(23) (a) Underwood, D. J.; Hoffmann, R.; Tatsumi, K.; Nakamura, A.; Yamamoto, Y. *J. Am. Chem. Soc.* **1985**, *107*, 5968. (b) Mealli, C. *J. Am. Chem. Soc.* **1985**, *107*, 2245.
(24) Cabeza, J. A.; Lahoz, F. J.; Martin, A. *Organometallics*, **1992**, *11*, 2754.
(25) (a) Matsuda, H.; Ayabe, Y. *Z. Electrochem.* **1955**, *59*, 494. (b) Nicholson, R. S. *Anal. Chem.* **1965**, *37*, 1351.
(26) Marcus, R. A. *J. Chem. Phys.* **1965**, *43*, 679 and references therein.
(27) Rimmelin, J.; Lemoine, P.; Gross, M.; de Montauzon, D. *Nouv. J. Chim.* **1983**, *7*, 453 and references therein.

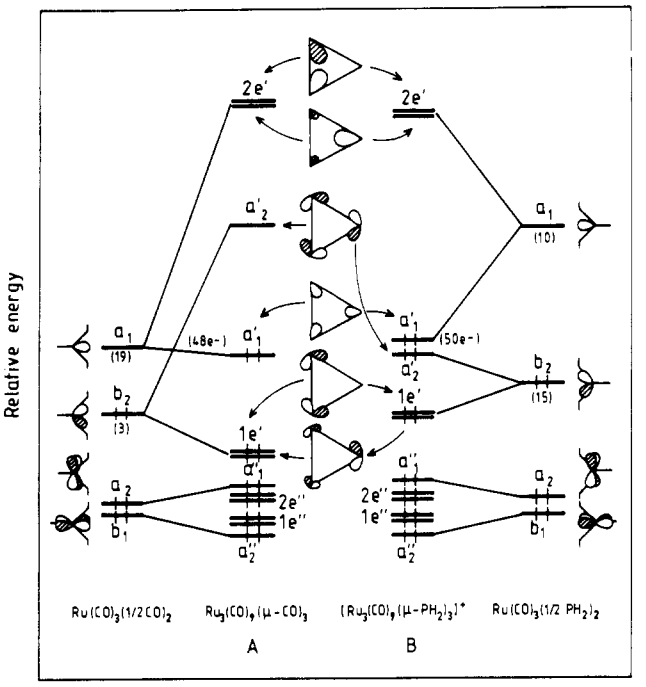

Figure 4. Qualitative MO diagrams for the 48-e D_{3h} model **A** (left) and for the 50-e D_{3h} model **B** (right), generated from the assemblage of three $Ru(CO)_3L'_2$ units. Numbers in parentheses indicate the percentage bridging ligand character.

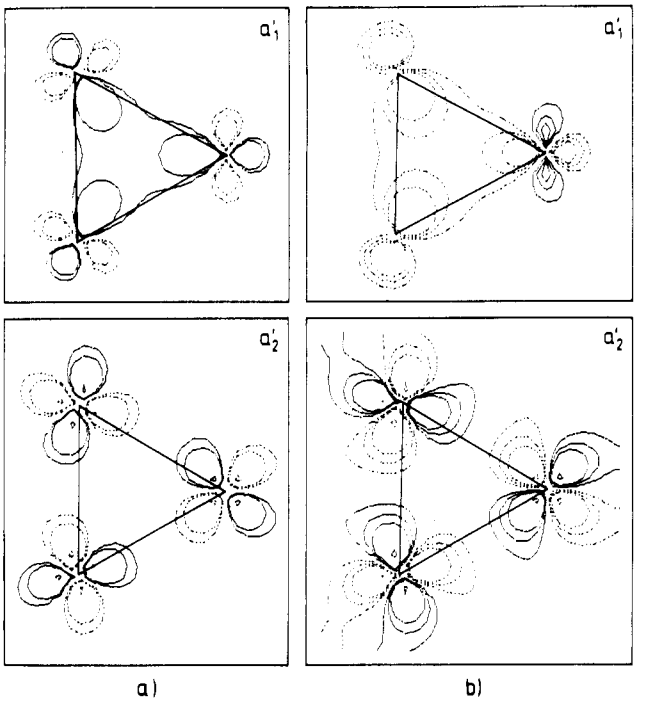

Figure 5. Contour maps in the metallic plane for the a'_1 and a'_2 MO's of model **B** (a) and their corresponding ones in the complex $Ru_3(\mu_3\text{-}\eta^2\text{-}P(C_6H_5)(C_5H_4N))(\mu\text{-}P(C_6H_5)_2)_3(CO)_6$ (**9**) (b).

can be simply considered to consist of one d^6 $ML_3L'_2$ and two d^6 $ML_2L'_3$ fragments of D_{3h} pseudosymmetry. L is a terminal two-electron σ-donor ligand and L' represents a two-electron σ-donor ligand equivalent to half a bridging carbonyl dianion or a bridging phosphido monoanion group.[28] The splitting of the metallic d-levels for a d^6 $Ru(CO)_3L'_2$ is shown on the left-hand side of Figure 4 in the case of $L' = {}^1/_2(CO)^{2-}$ and on the right-hand side in the case of $L' = {}^1/_2(PH_2)^-$. The orbital scheme, two below two, is reminiscent of that encountered for a d^6 D_{3h} ML_5 entity.[29] Among the four d-levels shown in Figure 4, the two lowest (noted b_1 and a_2 in the real C_{2v} symmetry) of π and δ symmetry respectively, are almost purely metallic in character and stay almost unperturbed whatever the ligand L' is. On the other hand, replacement of the π-acceptor bridging CO's by the π-donor phosphido groups modifies somewhat the energy and the shape of the π-symmetry b_2 frontier molecular orbital (FMO). It is slightly destabilized in energy when the bridging CO ligands are substituted by the phosphido ligands. The major change concerns its bridging ligand percentage character, which increases from 3% with CO to 15% with PH_2. Noticeably, the σ FMO, noted as a_1, is destabilized in the case of the phosphido bridges. In both cases however, participation of the bridging ligand is important in that orbital.

When three d^6 $Ru(CO)_3L'_2$ fragments are brought together, a D_{3h} model, $Ru_3(CO)_9(L'_2)_3$, is obtained. The molecular orbital diagrams of the two models $Ru_3(CO)_9(\mu\text{-}CO)_3$ (**A**) and $Ru_3(CO)_9(\mu\text{-}PH_2)_3$ (**B**) made of the assemblage of three $Ru(CO)_3(\mu\text{-}{}^1/_2CO)_2$ and $Ru(CO)_3(\mu\text{-}{}^1/_2PH_2)_2$ are shown in the middle of Figure 4. In both **A** and **B**, the two lower orbitals of the three metallic moieties, b_1 and a_2, interact very little to generate a low-lying set of six filled molecular orbitals (MO), labeled as a''_2, 1e'', 2e'' and a''_1 in D_{3h} symmetry. The σ-hybrid orbitals a_1 of each d^6 $ML_3L'_2$ fragment interact strongly to give rise to one bonding MO, a'_1, and two highly antibonding orbitals, noted as 2e' in Figure 4. The interaction of the b_2 FMO's of the three metallic fragments leads to the formation of one bonding component, 1e', and one antibonding component, a'_2. In **A**, the

Chart I

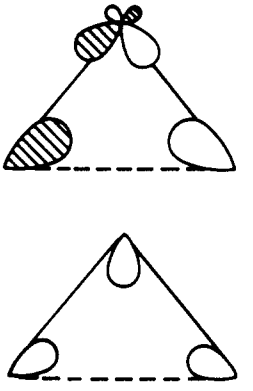

a'_2 MO is strongly antibonding and therefore lies high in energy, largely above the bonding upper orbital a'_1. For a 48-electron count, the bonding and nonbonding MO's are filled, whereas the antibonding ones are empty. The six electrons housed in the 1e' and a'_1 orbitals are responsible for the existence of the three formal single metal–metal bonds in **A**. This bonding scheme is analogous to that observed for the 48-electron trimer $Os_3(CO)_{12}$.[30]

With phosphido bridges instead of carbonyl bridges, the a'_2 MO, which derives from the b_2 FMO, is less metallic in character than its corresponding one in **A**. Consequently, it is less metal–metal antibonding and lies just below the a'_1 MO. The occupation of the slightly bonding 1e' levels and their unique antibonding counterpart a'_2 leads to an overall nonbonding effect. Therefore, only the a'_1 HOMO is responsible for the M–M bonding in the 50-e model **B**. This two-electron-three-center delocalized picture leads to an enhancement of the metal–metal bond lengths in this new 50-e species. The situation is reminiscent of the one encountered in H_3^+.[31]

Although the complexes $Ru_3(\mu_3\text{-}\eta^2\text{-}P(C_6H_5)(C_5H_4N))(\mu\text{-}P(C_6H_5)_2)(\mu\text{-}CO)_2(CO)_6$ (**4**) and $Ru_3(\mu_3\text{-}\eta^2\text{-}P(C_6H_5)(C_5H_4N))(\mu\text{-}P(C_6H_5)_2)_3(CO)_6$ (**9**) exhibit C_1 and C_s symmetry respectively,

(28) Evans, D. G. *J. Chem. Soc., Chem. Commun.* **1983**, 675.
(29) Rossi, A.; Hoffmann, R. *Inorg. Chem.* **1975**, *14*, 365.
(30) Schilling, B. E. R.; Hoffmann, R. *J. Am. Chem. Soc.* **1979**, *101*, 3436.
(31) Albright, T. A.; Burdett, J. K.; Whangbo, M.-H. In *Orbital Interactions in Chemistry*, Wiley: New York, 1985.

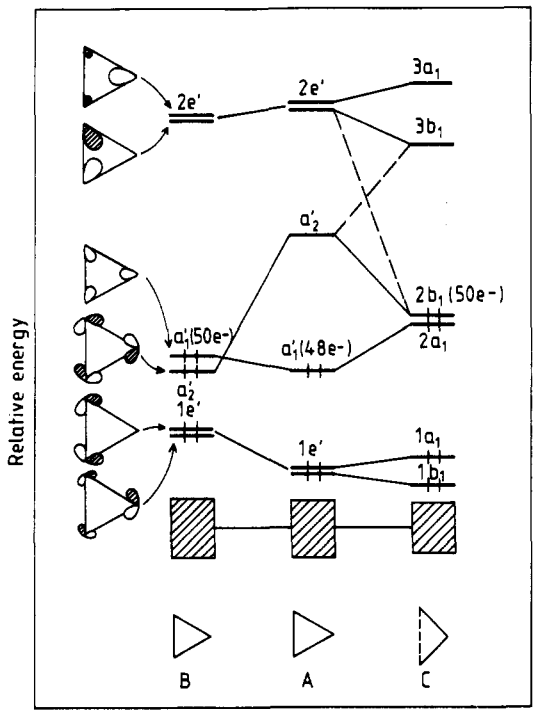

Figure 6. Qualitative comparison of the MO diagrams of models D_{3h} **A** (48 e), D_{3h} **B** (50 e), and C_{2v} **C** (50 e). The crosshatched boxes correspond to the six lowest levels shown in Figure 4.

a D_{3h} pseudosymmetry is retained for the metallic core. Indeed, the electronic structures of the 48-electron complex **4** and the 50-electron cluster **9** are respectively comparable to that of models **A** and **B**. Let us note for instance, the similarity between the two upper filled MO's of **9**, plotted in Figure 5, with the a'_1 and a'_2 MO's of model **B**. The lengthening of the metal–metal bonds in **9** compared to that of **4** (ca. 3.10 Å against ca. 2.82 Å) is due to the occupation of the antibonding a'_2-like MO in **9**.

A HOMO–LUMO gap of 1.49 eV is computed for the 50-e species **9**, while 0.88 eV separates the HOMO from the LUMO in the 48-electron compound **4**. The presence of the LUMO in **4** at relatively low energy and in the middle of a large energy gap (0.88 eV below and 1.21 eV above) suggests that it might be possible to reduce complex **4** and thus obtain a 50-e species isostructural to compound **9**.

Contrary to complex **9**, the 50-e species $Ru_3(\mu_3\text{-}\eta^2\text{-}P(C_6H_5)\text{-}(C_5H_4N)(\mu\text{-}P(C_6H_5)_2)(CO)_9$ (**5**), resulting from the addition of CO to complex **4**, adopts the usual open geometry (see eq 2). It can be regarded as consisting of one d^8 ML_4 and two d^7 $ML_3L'_2$ fragments. Calculations performed on the closed 50-e model $Ru_3(CO)_{12}(\mu\text{-CO})$, which derives from model **A** by replacing two bridging CO's by three terminal ones, show some instability if the closed geometry is retained. It is the main reason why a more open structure is preferred for the 50-e species: a lengthening of the metal–metal bond spanned by the bridging CO group prevents short CO–CO nonbonding contacts. Consequently, a stabilization is observed upon rearrangement, and the four bonding electrons responsible for the metal–metal bonding in the C_{2v} open cluster $Ru_3(CO)_{12}(\mu\text{-CO})$, **C**, are then located in the two MO's schematically represented in Chart I. The $2a_1$ orbital derives from the a'_1 MO present in the MO diagram of **A** (see Figure 6). The $2b_1$ MO results from the stabilization of one component of the 2e' set, strongly mixed with the a'_2 component.

The conclusions drawn above for **C** can be applied to the compound $Ru_3(\mu_3\text{-}\eta^2\text{-}P(C_6H_5)(C_5H_4N))(\mu\text{-}P(C_6H_5)_2)(CO)_9$ (**5**). An important HOMO–LUMO gap of 1.69 eV is obtained for the open structure **5**, with the observed 50-e count. It is noteworthy that most 50-e trimetallic systems exhibiting an open geometry are also based on one d^6 ML_4 and two d^7 ML_5 entities.[32]

Acknowledgment. Financial support from the CNRS is gratefully acknowledged. We also wish to thank Dr. Cabeza for personal communication of his work (ref 24).

Supplementary Material Available: Tables of crystal data and anisotropic thermal parameters (2 pages). Ordering information is given on any current masthead page.

(32) For a review on transition metal clusters exhibiting open metal polyhedra, see: Albers, M. O.; Robinson, D. J.; Coville, N. J. *Coord. Chem. Rev.* **1986**, *69*, 127.